

# P13.15 The effect of a wet radome on dualpol data quality

Michael Frech\*

Deutscher Wetterdienst

Hohenpeissenberg Meteorological Observatory, Germany

## 1. Introduction

Operational radar systems typically are equipped with a radome. A radome protects the radar system and allows continuous operation under all weather conditions. The potential disadvantage of using a radome is that it may affect the outgoing and incoming microwave, in particular when the radome is wet. Radomes are typically optimized to minimize the transmission loss and to avoid azimuthal variations of the received signal due to radome seams. Furthermore, the radome material is chosen to be hydrophobic, in order to avoid as much as possible additional attenuation due to a wet radome surface. Radome attenuation is discussed in a number of papers where the effect typically is analyzed under idealized conditions (e.g. Manz, 2001). The level of attenuation will also depend on rainfall intensity and type. The dependence on rainfall intensity has been investigated recently in Kurri and Huuskonen (2008). Under operational conditions, the attenuation of the radar signal may depend on elevation and azimuth. For example, attenuation may be quite heterogeneous under strong wind conditions because the radome is not equally wet (e.g. Germann (2000)). The effect wet radome attenuation on polarimetric moments so far has not been investigated in detail.

In this work we investigate the effect of radome attenuation on polarimetric moments under operational conditions. Data are taken from the dualpol C-band radar at the Hohenpeissenberg Meteorological Observatory. This radar is the research radar of the German Met.

---

\*Corresponding author address: Michael Frech, DWD, Meteorologisches Observatorium Hohenpeissenberg, D-82383 Hohenpeissenberg, Germany. Email: Michael.Frech@dwd.de  
Extended abstract, AMS Radar conference 2009, Williamsburg, VA.

Service, DWD. The radar is protected by a 12-year old radome of orange-peel type. No dedicated maintenance has been applied to this radome.

Eleven months of radar data are analyzed and statistics are computed to identify the mean attenuation of a wet radome and its variability. Variability may be expected due to the meteorological conditions at the radar site (e.g. wind) or due to the type of hydrometeors (e.g. snow vs. rain).

## 2. The data

Data from February to December 2008 are analyzed. We perform 5 minute volume scans in STAR (Simultaneous Transmitt and Receive) mode. In STAR mode, each volume contains 10 elevation angles. The main characteristics of the scan definition are briefly described here:

**STAR-Mode (every 5 min)**, with the following settings:

- 10 elevation angles: 0.5°, 1.5°, 2.5°, 3.5°, 4.5°, 5.5°, 8°, 12°, 17°, 25°
- elevation angles 0.5 - 4.5°:  $PRF = 640$  Hz, AZ-rate  $16^\circ/s$ , range= 230 km.
- elevation angles 5.5 - 25°:  $PRF = 1160$  Hz, AZ-rate  $16^\circ/s$ , range= 128 km.
- Raw-range bin resolution: 125 m
- Range averaging: 250 m.
- pulse width:  $0.8 \mu s$
- Dynamic angle synching (DAS) with  $1^\circ$  ray width.

- The following moments are available:  
 $CZH, CZV, UZH, UZV, VH, VV, WH, WV,$   
 $\Phi_{DP}, Z_{DR}, \rho_{HV}, K_{DP}$ , with  
 $CZH, CZV$ : clutter corrected reflectivity factor  
 $Z$ , horizontal ( $H$ ) and vertical ( $V$ ) polarization.  
 $UZH, UZV$ : un-corrected reflectivity factor  $Z$ ,  
horizontal ( $H$ ) and vertical ( $V$ ) polarization.  
 $VH, VV$ : line-of-sight Doppler velocity, from  
horizontal ( $H$ ) and vertical ( $V$ ) polarization.  
 $WH, WV$ : Doppler spectral width, from hori-  
zontal ( $H$ ) and vertical ( $V$ ) polarization.  
 $Z_{DR}$ : Differential reflectivity.  
 $\Phi_{DP}$ : Differential phase.  
 $K_{DP}$ : Specific differential phase.  
 $\rho_{hv}$ : Cross-correlation coefficient.

The reference precipitation measurement is a rain gauge at the radar site. These data with one-minute resolution are used to define the onset and end of a precipitation event over the site. Furthermore, the independent precipitation data allow the classification of the attenuation effect with respect to precipitation rate.

### 3. Case study with moderate precipitation

Two screenshots of  $Z_{DR}$  taken 25.4.2008 just before and during precipitation at the radar site are shown in Figure 1. The situation was characterized by strong graupel showers. From literature (e.g. Bringi and Chandrasekar, 2001) it is known that graupel is typically characterized by slightly negative or near zero  $Z_{DR}$  which is consistent with the  $Z_{DR}$ -values before the precipitation reaches the radar site. During the precipitation event at the site,  $Z_{DR}$  becomes positive which can be attributed to differential radom attenuation of  $Z_H$  and  $Z_V$  because the character of precipitation (graupel) did not change. A more quantitative impression on the magnitude of attenuation is shown in Figure 2. Here we compute sweep averages of radar moments at  $el = 1.5^\circ$ . In order to reduce scatter due to bad signal quality and clutter we only consider data at  $r > 4$  km,  $\rho_{HV} > 0.8$  and  $z < 12000$  m. We

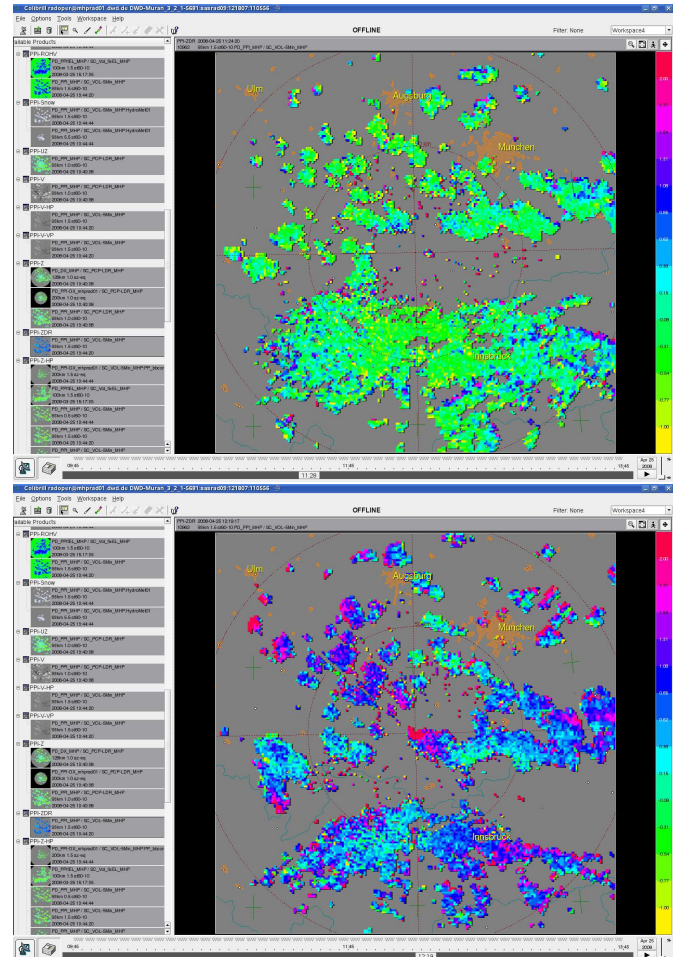


Figure 1:  $Z_{DR}$  [dB] screenshots taken 25.4.2008 before the precipitation event reaches the site (left) and while the event is over the site (right). The scale of  $Z_{DR}$  is from -1 (yellow) to +2 (red).

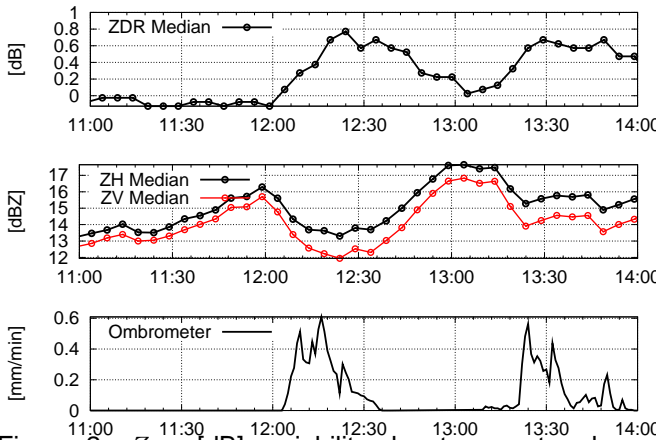


Figure 2:  $Z_{DR}$  [dB] variability due to a wet radome. Before the precipitation reaches the radar site,  $Z_{DR}$  is slightly negative. During the precipitation event  $Z_{DR}$  becomes positive ( $Z_{DR} \approx 0.8$ ).

make the assumption that there is no overall change in precipitation type and intensity as seen by the radar. As such, any variations are attributed to the radome effect. As a reference we show the rain-gauge measurements at the radar site. Once the precipitation reaches the site, we notice a decrease of  $Z_H$  and  $Z_V$  of about 3 and 4 dB, respectively.  $Z_V$  attenuation is stronger which is highlighted by the increase of  $Z_{DR}$  up to a value of 0.8 dB. Stronger  $Z_V$  attenuation can be attributed to the more or less vertically aligned water runoff from the radome. From Figure 2 we can also deduce a drying time of the radome on the order of 30 min which can be related to the time it takes to reach again the magnitudes of the radar moments as observed just before the precipitation event reaches the site. RHOHV shows a weak decrease (not shown) and there is no clear picture seen in PHIDP

#### 4. Case study with intense precipitation

As another example we consider an event of very intense precipitation (up to 4 mm/min) observed on 17.5.2008. We again show two screenshots of radar products before and while the cell is over the radar site (Figure 3). Note

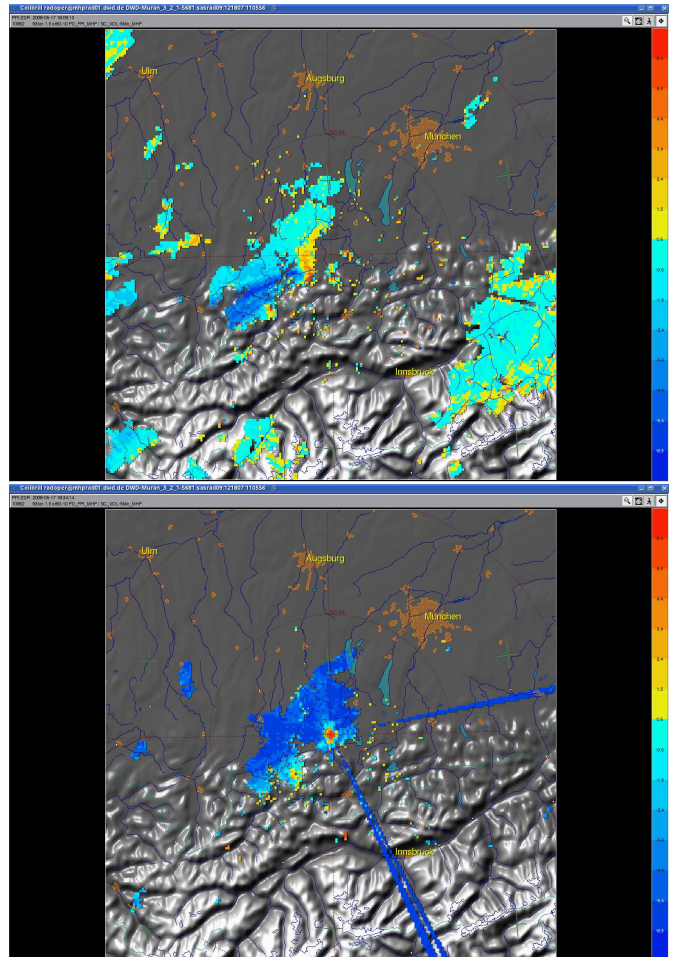


Figure 3:  $Z_{DR}$  [dB] screenshots taken 17.5.2008 before the precipitation event reaches the site (left) and while the event is over the site (right), 17.5.2008. The scale of  $Z_{DR}$  is from -6.4 (blue) to +6.4 (red). Zero  $Z_{DR}$  coded with as yellow.

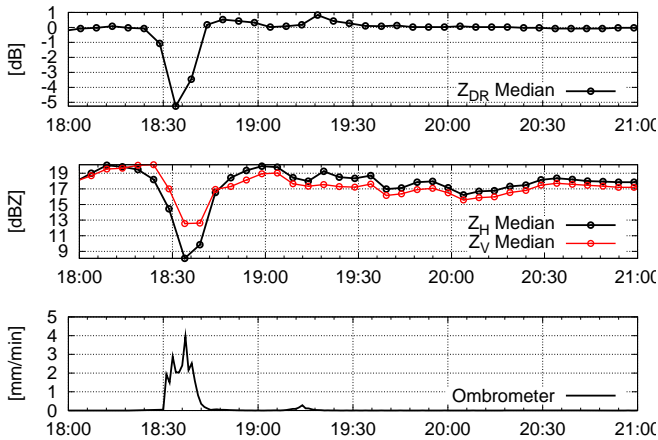


Figure 4:  $Z_{DR}$  [dB] bias during an intense precipitation event.

that we use a different color scale compared to the one of Figure 1. There are a number of features readily visible from Figure 3. First of all we see strong attenuation effects in  $Z_{DR}$  (blue colors behind the leading edge of the cell south-west from the radar site). The leading edge of the cell is characterized by large positive  $Z_{DR}$  values (up to +5 dB) which is indicative of large drop sizes including possibly hail. This corresponds to drop sizes of  $\approx 6 - 8$  mm (Bringi and Chandrasekar, 2001). When the cell is over the site,  $Z_{DR}$  assumes large negative values ( $\approx -5$  to  $-4$  dB). We furthermore observe ray-shaped disturbances when the cell is over the site. Those disturbances appear to be not coherent, as they are not visible in the Doppler moments. The source of those echos appears related to a shielding problem which has been fixed in the meanwhile. Similar to the previous case we compute sweep averaged values of each radar moment, in order to quantify the relative magnitude changes for each moment. The time series of  $Z$ ,  $Z_{DR}$  and ombrometer data (Figure 4) substantiate the more qualitative view of the screenshots (Figure 3). Here we find a strong negative bias in  $Z_{DR}$ . The attenuation of  $Z_H$  is significantly stronger than for  $Z_V$ . The overall attenuation of  $Z_H$  is on the order of 10 dB which is due to a combination of the wet radome effect and the path attenuation by the cell itself. A large negative  $Z_{DR}$  deviation is already observed before the precipitation reaches the site. The contribution of the wet radome to the  $Z_{DR}$  bias is difficult

to quantify in this case. The data suggest that the micro-physical structure of the cell and the associated attenuation dominate the (negative)  $Z_{DR}$  bias. This is different from the previous case where we find positive  $Z_{DR}$ . The weak/moderate precipitation event starting around 19:15 UTC shows a positive  $Z_{DR}$  bias consistent with the previous case study.

## 5. Statistical analysis

### a. Bias as a function of time

We analyze the effect of radome attenuation considering all precipitation events from February to December 2008. The data sample is expected to be rather heterogeneous so we initially define criteria to isolate specific precipitation events from the data. We only consider precipitation events that have at least a duration of 10 minutes. Furthermore, we require a period of 30 minutes without any precipitation at the radar site prior the precipitation event. The 30 minute sequence is defined as the dry radome reference where radar data is expected to be affected solely by the radome design characteristics. Applying these criteria to the data we obtain about 70 samples for further analysis which is still a rather small sample size for a statistical analysis. Nevertheless we perform some basic analysis in order to identify basic properties of the radome attenuation effect. For these samples, the average accumulated rain and its range is shown in Figure 5. In the following we consider only the first 30 minutes after the beginning of a precipitation event. The analysis is carried for four elevation angles:  $0.5^\circ$  (sweep 9),  $1.5^\circ$  (sweep 8),  $2.5^\circ$  (sweep 7) and  $8^\circ$  (sweep 3).

The corresponding relative change of  $Z_{DR}$  as a function of time is shown in Figure 6 for sweep 8. This moment is impacted most by a wet radome. The  $Z_{DR}$  bias increases initially more or less linearly for the first 20-30 minutes before maximum attenuation for a given rain event is reached. The average differential attenuation is +0.3 dB. Considering a required accuracy of 0.1 dB for  $Z_{DR}$ , wet radome attenuation has to be considered and should be corrected for in operational applications. The spread in  $Z_{DR}$  bias suggests that the bias is dependent on the actual rain rate and other meteorological effects which may lead to a heterogeneous wetting of

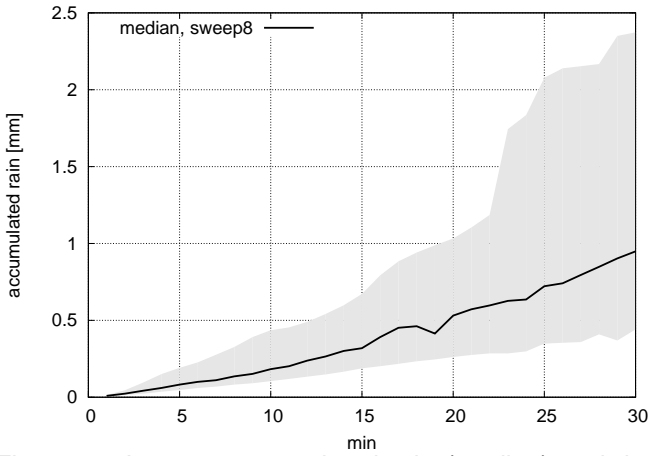


Figure 5: Average accumulated rain (median) and the distribution of rain amounts for the samples to study radom attenuation. The range is defined by the 1st and third quartile of the distribution at a given time.

the radome. The dependence on rain rate will be investigated in the next section.

For illustrative purposes we show also the variation of  $\rho_{hv}$  which does not show a comparable systematic behaviour as a function event time (Figure 7). Here deviations on the order of 0.002 are observed due to radome attenuation which is smaller than the required accuracy (0.005) but which adds to the overall uncertainty in  $\rho_{hv}$  from other components in the radar system.

#### b. Bias as a function of elevation angle

In principle, the influence of wet radome may be elevation dependent as the water coating of the radome will be variable. This may be due to variable exposure of a radome element to the precipitation event, e.g whether it is up or downstream of the main atmospheric flow. This is an aerodynamic effect which may cause variable radome water coating as a function of azimuth and elevation. Furthermore an elevation dependent water coating can be expected as more and more water is collected while the water drains off from the radome due to gravitation. This water runoff is collected in little streams which may cause an additional azimuthal dependence in attenuation. In principle, the analysis of the elevation dependence could take into account wind speed as a further

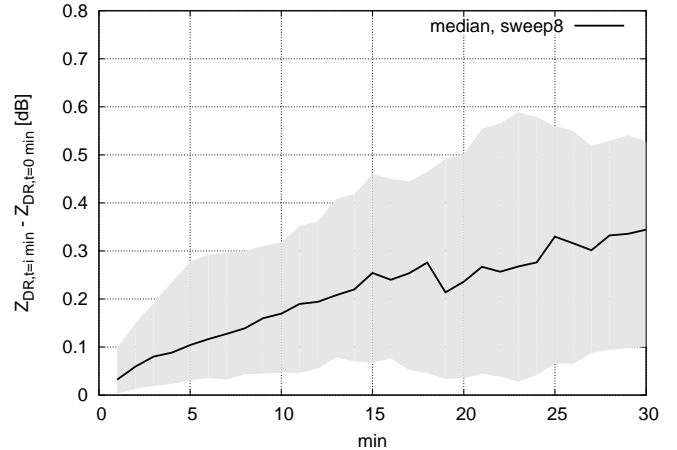


Figure 6:  $Z_{DR}$  change relative to the average "dry"  $Z_{DR}$  [dB].

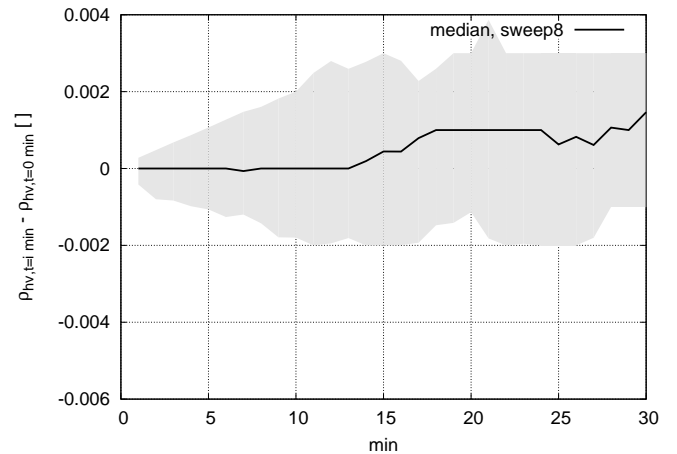


Figure 7:  $\Phi_{dp}$  and  $\rho_{hv}$  change relative to the average "dry" values.

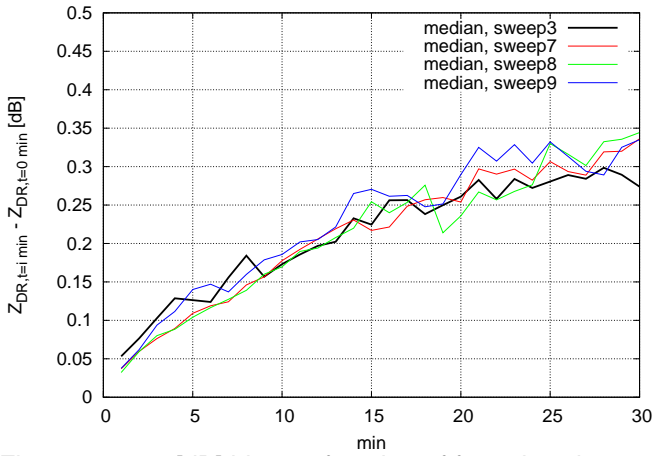


Figure 8:  $Z_{DR}$  [dB] bias as function of four elevation angle: sweep 3 ( $8^\circ$ ), 7 ( $2.5^\circ$ ), 8 ( $1.5^\circ$ ) and 9 ( $0.5^\circ$ ).

variable. This may be considered at a later stage of the analysis when a larger data set is available.

The analysis of the four elevation angles shows no distinct differences for  $Z_{DR}$  (Figure 8). This would suggest an elevation independence of  $Z_{DR}$  attenuation at least for the sample considered here.

### c. Bias as a function of rain rate

Previous case studies show that the bias is a function of rain rate. We therefore analyse the sample with respect to rain rate focusing on  $Z_{DR}$ . The results are shown in Figure 9

Up to a rain rate of  $\approx 0.15$  mm/min, there is a steady increase of  $Z_{DR}$  bias up to a level of 0.6 dB. On average, this bias remains constant for larger rain rates (saturation effect). The scatter is relatively large for larger rain rates due to a small sample size. Since our sample also includes a number of snow cases, we carried out a sensitivity study by removing the snow samples. The result is shown in Figure 10. Snow cases are mainly related to small precipitation rates. Removing those samples leads a more or less linear bias increase as a function of rain rate (up to  $\approx 0.1$  mm/min). This feature may be used for a correction scheme to correct for the  $Z_{DR}$  bias.

We also analyze the dependence of RHOHV on rain rate. The result is shown in Figure 11. There is no clear trend visible. At large rain rates there appears to be a

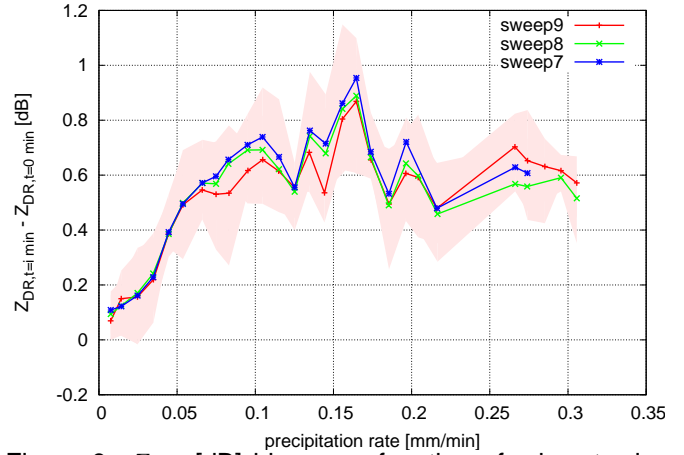


Figure 9:  $Z_{DR}$  [dB] bias as a function of rain rate, including snow cases. Shown is the bias at lower elevation angles.

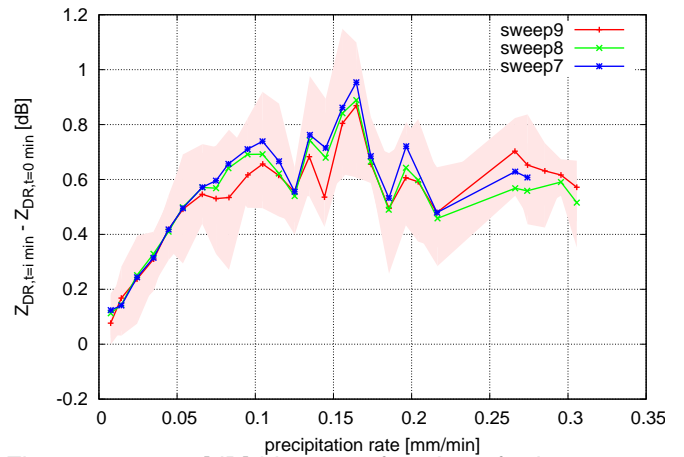


Figure 10:  $Z_{DR}$  [dB] bias as a function of rain rate, excluding snow cases. Shown is the bias at lower elevation angles.

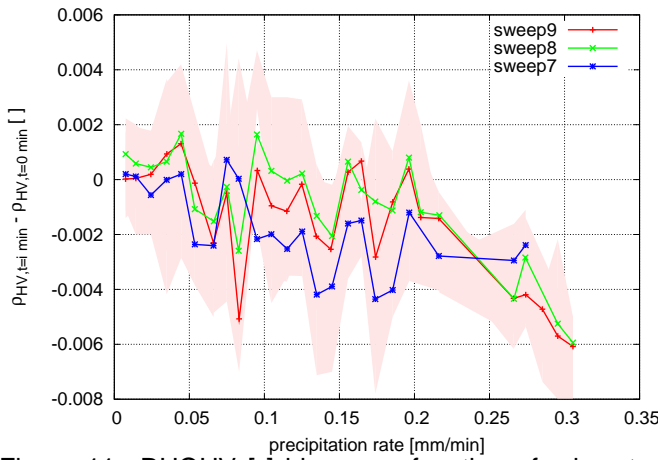


Figure 11: RHOHV [ ] bias as a function of rain rate. Shown is the bias at lower elevation angles.

bias towards smaller RHOHV values, but on average the magnitudes are small and still within the target accuracy.

## 6. Summary

In this paper we have analyzed the impact of a wet radome on dualpol moments. The largest impact is identified for  $Z_{DR}$ . We have shown that there can be significant bias in  $Z_{DR}$  as a function of rain rate. The bias can be as high as +0.8 dB or more. Algorithms (HMC, QPE) that rely on  $Z_{DR}$  are certainly affected by such a bias. A correction of  $Z_{DR}$  appears necessary. Other dualpol moments such as RHOHV and PHIDP appear, at least for our samples, weakly affected by a wet radome.

The  $Z_{DR}$  bias as a function of rain rate basically shows a linear increase up to a rain rate of  $\approx 0.1 - 0.15$  mm/min.

The observed bias is due to a 12 year old orange-peel radome that has never been maintained. In that respect, the results emphasize the necessity of high quality hydrophobic surface coating and the consideration of preventive radome maintenance to minimize the impact of a radome on dualpol moments (in particular the differential moments). The presented results serve as a reference data set against which the radomes of the new DWD weather radar systems will be evaluated.

## References

- Bringi, V. N. and V. Chandrasekar: 2001, *Polarimetric Doppler Weather Radar*. Cambridge University Press, 636 pp.
- Germann, U.: 2000, *Spatial continuity of precipitation, profiles of radar reflectivity and precipitation measurements in the Alps*. Ph.D. thesis, Swiss Federal Institute of Technology (ETH), Zürich.
- Kurri, M. and A. Huuskonen: 2008, Measurements of the transmission loss of a radome at different rain intensities. *J. Atmos. Ocean. Tech.*, **25**, 1590 – 1599.
- Manz, A.: 2001, Radome influence on weather radar systems, principles and calibration issues. *AMS Workshop Radar Calibration, Albuquerque, NM, USA*, p8.